Hypernetted-chain Euler-Lagrange equations and the electron fluid

John G. Zabolitzky*
Argonne National Laboratory, Argonne, Illinois 60439
(Received 14 January 1980)

Least upper bounds to the ground-state energy of the electron fluid are obtained by solving Euler-Lagrange equations obtained within the framework of Fermi hypernetted-chain theory for arbitrary density and spin polarization. It is shown that the so-obtained approximate distribution and structure functions satisfy known exact relations in the high- and low-density limits as well as in the long-wavelength limit at any density. The numerical results are in excellent agreement with coupled-cluster perturbational and Monte Carlo type calculations. As a by-product a simple analytic solution accurate in the high-density limit is obtained which is superior to the random-phase approximation in the metallic density regime.

I. INTRODUCTION

The theory of the homogeneous electron fluid at zero temperature has received renewed interest in recent years since several new, powerful many-body techniques have become available. Noticeably there are variational Monte Carlo[1] results, variational results obtained within the Fermi hypernetted-chain approximation[2] as advocated by Fantoni and Rosati,[3] and a calculation using the coupled-cluster formalism.[4] Less recent theories and their results are discussed in Ref. 1. All of these works fall into either of two categories, variational or partially summed perturbational. The most advanced treatment falling into the latter category may be found in Ref. 4. The present paper continues investigations within the first category.

Though admittedly the homogeneous fluid is a rather crude approximation to real physical systems it has received renewed interest recently since it provides the input necessary for the local-density[5] and local-spin-density[6] formalisms. It is one of the main purposes of the present paper to obtain as accurately as possible the required correlation energy as a function of both density and spin polarization. Furthermore, one may study some interesting phenomena, e.g., phase transitions[1] in this model. Moreover, since virtually every many-body method has been applied to this model it serves as another benchmark for many-body theories. Within the latter context it is to be noted that theories[1–4] previously have been applied mainly to problems involving *short-range forces*. The electron fluid with its *long-range* Coulomb force is therefore an interesting test case useful to study the long-wavelength behavior of the various many-body theories. This latter question is of special importance since there is a long-standing controversy[7] about the treatment of antisymmetry, i.e., exchange effects in Jastrow variational calculations employing the hypernetted-chain approximation, which is specifically concerned with a long-wavelength discrepancy.

In Sec. II I will derive expressions for the variational energy expectation value which upon functional variation will yield Euler-Lagrange equations for the correlation factor describing the wave function. Special care will be taken to preserve certain exact properties in spite of the approximations necessary.

In Sec. III numerical results are presented for a variety of densities and spin polarizations. Numerical checks are made to validate the approximations introduced in Sec. II. My findings are summarized in Sec. IV.

II. VARIATIONAL THEORY

A. Energy expectation value

Let us consider a variational wave function of the Jastrow type[8]

$$\psi(\vec{r}_1, \ldots, \vec{r}_N) = F\phi = \prod_{i<j} f(r_{ij})\phi \quad , \tag{1}$$

where F is a symmetric correlation operator and ϕ a determinant of plane waves rendering ψ antisymmetric. This kind of wave function has been used very successfully in a wide variety of many-body problems though it has known disadvantages. Most restrictive is the use of a state-independent correlation factor $f(r)$ not depending on the momenta of the particles. This will give the same two-body correlations for particles on the Fermi surface and in the center of the Fermi sphere. Less important, three-body correlations other than products of two-body correlations are excluded. The latter point probably is of very little importance for the electron fluid since it has been found[9] that three-body correlations of

other than product form are important only for very hard interactions like Lennard-Jones. Furthermore, the correlation factor is the same for spin-parallel and spin-antiparallel pairs of electrons. This is not as important a shortcoming as one might fear on first sight. Since the Hamiltonian is spin independent, evaluation of the energy implies an average over spin projections. Using a spin-independent correlation factor may be interpreted as taking the average of the spin-parallel and spin-antiparallel correlation factors first and then evaluating the energy which should not make much of a difference (see below also).

In this section I will derive approximate expressions for the variational energy per particle

$$E_{\text{var}}=\frac{1}{N}\frac{\langle\psi|H|\psi\rangle}{\langle\psi|\psi\rangle} \tag{2}$$

for a given wave function (1). In the next section this energy will be functionally minimized within the space given by the ansatz (1).

The Hamiltonian appropriate for the homogeneous electron fluid is

$$H=T+V=-\frac{\hbar^2}{2m}\sum_i\nabla_i^2+\sum_{i<j}\sum_{h\neq 0}\frac{4\pi e^2}{\Omega k^2}e^{i\vec{k}\cdot(\vec{r}_i-\vec{r}_j)}$$

$$=\sum_i t_i+\sum_{i<j}v(r_{ij}) \ , \tag{3}$$

where m is the electron mass and Ω the volume. I will consider N particles in volume Ω and eventually take the limit $N,\Omega\to\infty$ at constant density $\rho=N/\Omega$. The exclusion of $k=0$ in the last term of Eq. (3) serves to subtract the positive background. The two-body radial distribution function is defined as[10]

$$g(r_{12})=\frac{N(N-1)}{\rho^2}\frac{\int d^3r_3,\ldots,d^3r_N|\psi(\vec{r}_1,\ldots,\vec{r}_N)|^2}{\int d^3r_1,\ldots,d^3r_N|\psi(\vec{r}_1,\ldots,\vec{r}_N)|^2} \ . \tag{4}$$

The potential energy therefore is given by[10]

$$\frac{\langle V\rangle}{N}=\tfrac{1}{2}\rho\int d^3r\,v(r)[g(r)-1] \ , \tag{5}$$

where the subtraction of 1 comes from the background subtraction. The structure function $S(k)$ is defined by[10]

$$S(k)-1=\rho\int d^3r[g(r)-1]e^{i\vec{k}\cdot\vec{r}} \ . \tag{6}$$

Therefore an alternative form for the potential energy is

$$\frac{\langle V\rangle}{N}=\frac{1}{2(2\pi)^3}\int d^3k\frac{4\pi e^2}{k^2}[S(k)-1] \ . \tag{7}$$

The three-body radial distribution function is given by[10]

$$g_3(\vec{r}_{12},\vec{r}_{23})=\frac{N(N-1)(N-2)}{\rho^3}\frac{\int d^3r_4,\ldots,d^3r_N|\psi(\vec{r}_1,\ldots,\vec{r}_N)|^2}{\int d^3r_1,\ldots,d^3r_N|\psi(\vec{r}_1,\ldots,\vec{r}_N)|^2} \ . \tag{8}$$

The expectation of the kinetic energy may then be written[11–13]

$$\frac{\langle T\rangle}{N}=T_\phi+T_2+T_3$$

$$=\frac{3}{5}\frac{\hbar^2}{2m}k_F^2+\rho\int d^3r g(r)\frac{\hbar^2}{2m}[\nabla\ln f(r)]^2+\rho^2\int d^3r_{12}\int d^3r_{23}g_3(\vec{r}_{12},\vec{r}_{23})\frac{\hbar^2}{2m}\vec{\nabla}_2\ln f(r_{12})\cdot\vec{\nabla}_2\ln f(r_{23}) \ , \tag{9}$$

after a partial integration. Note that no explicit reference is made to the determinantal part of the wave function (1), except for the trivial term T_ϕ. In Eq. (9), T_ϕ denotes the free Fermi-gas kinetic energy, and k_F is the Fermi momentum

$$\rho=sk_F^3/6\pi^2 \ ,$$

where s denotes the degeneracy ($s=2$ for the unpolarized Fermi fluid, $s=1$ for the totally spin-polarized fluid). It is to be noted that in order to obtain Eq. (9) a specific choice was made in doing partial integrations.[12,13] This version of the kinetic energy has been termed the Clark-Westhaus (CW) form. There are other equivalent forms to calculate the kinetic energy expectation value, the usefulness of which will be discussed below. One good reason to use the CW form for the kinetic energy is that in all previous studies[12,13,15] it has always been found to *over*estimate the energy and never *under*estimate it as some other forms do if one invokes approximations to the energy expectation value. Therefore, we are confident that the upper-bound property of the variational energy, Eq. (2), is still preserved in an approximate calculation if one uses the CW form. It is evident from Eqs. (6) and (9) that in order to evaluate the energy expectation value (2) exactly for given wave function (1) it suffices to know the two- and three-body radial distribution functions. Let me temporarily consider a simpler wave function than Eq. (1), namely, a sym-

metric (Bose) wave function obtained by setting $\phi = 1$,

$$\psi(\vec{r}_1, \ldots, \vec{r}_N) = \prod_{i<j} f(r_{ij}) \quad . \tag{10}$$

For this wave function, invoking the hypernetted-chain (HNC) *expansion*, we have rigorously[10]

$$u(r) = \ln g(r) - \frac{1}{\rho}\left[\frac{[S(k)-1]^2}{S(k)}\right]^F - E(r) \quad , \tag{11}$$

where the "pseudopotential" $u(r)$ is defined by

$$f(r) = \exp[\tfrac{1}{2}u(r)] \quad . \tag{12}$$

$[\,]^F$ denotes Fourier transform

$$\begin{aligned} a(r) &= [\tilde{a}(k)]^F = \frac{1}{(2\pi)^3}\int d^3k \tilde{a}(k) e^{-i\vec{k}\cdot\vec{r}} \quad , \\ \tilde{a}(k) &= [a(r)]^F = \int d^3r a(r) e^{i\vec{k}\cdot\vec{r}} \quad , \end{aligned} \tag{13}$$

and $E(r)$ is the sum of all elementary diagrams. The hypernetted-chain *approximation* consists simply of setting $E(r) = 0$. This approximation, originally invented for problems in statistical mechanics,[14] has been shown to be accurate for quantum problems not involving very strong repulsive potentials.[9,13,15]

Within this approximation, the two-body radial distribution function may be obtained by inverting Eq. (11). The three-body distribution function remains to be evaluated. It has been shown[10] that it may be expressed as a power series in the function

$$h(r) = g(r) - 1 \tag{14}$$

the first terms of which are

$$g_3(r_{12},r_{13},r_{23}) = 1 + h(r_{12}) + h(r_{23}) + h(r_{13}) \tag{15a}$$

$$+ h(r_{12})h(r_{13}) + h(r_{13})h(r_{23}) + h(r_{12})h(r_{23}) \tag{15b}$$

$$+ h(r_{12})h(r_{23})h(r_{13}) \tag{15c}$$

$$+ \rho\int d^3r_4 h(r_{14})h(r_{24})h(r_{34})\,[1 \tag{15d}$$

$$+ h(r_{12}) + h(r_{23}) + h(r_{13}) \tag{15e}$$

$$+ h(r_{12})h(r_{23}) + h(r_{13})h(r_{23}) + h(r_{12})h(r_{13}) \tag{15f}$$

$$+ h(r_{12})h(r_{23})h(r_{13})] \tag{15g}$$

$$+ \cdots \quad , \tag{15h}$$

where the terms (15h) not given have at least five factors h and two integrations over coordinates r_4, r_5 with two powers of the density. For practical purposes, the expansion (15) has to be truncated somewhere. Several versions of such truncations have been used[10]: (a) the Kirkwood superposition approximation is obtained if one retains (15a), (15b), and (15c) of Eq. (15); (b) the convolution approximation is obtained if terms (15a), (15b), and (15d) are retained. This approximation has the desirable feature of being consistent in the sense that the sequential relation

$$g(r_{12}) = \frac{\rho}{N-2}\int d^3r_3 g_3(\vec{r}_{12}, \vec{r}_{23}) \tag{16}$$

is satisifed, which is not true of *any* of the other approximations. (c) the HNC/4 approximation is obtained if terms (15a) through (15g) are retained.

I wish to rearrange Eq. (15) in order to use the convolution approximation as a first step, and evaluate corrections to it,

$$g_3(\vec{r}_{12}, \vec{r}_{23}) = g_3^{CA}(\vec{r}_{12}, \vec{r}_{23}) + g_3^{RES}(\vec{r}_{12}, \vec{r}_{23}) \quad . \tag{17}$$

where g_3^{RES} contains terms (15c) and (15e) to (15h) of Eq. (15). Using this decomposition, the kinetic energy expectation value may be written as

$$\frac{\langle T\rangle}{N}=T_\phi+T_2+T_3^{\mathrm{CA}}+T_3^{\mathrm{RES}}=\frac{3}{5}\frac{\hbar^2}{2m}k_F^2+\rho\int d^3r g(r)\frac{\hbar^2}{2m}\frac{1}{4}[\nabla u(r)]^2$$
$$+\rho^2\int d^3r_{12}\int d^3r_{23}\frac{\hbar^2}{8m}\vec{\nabla}_2u(r_{12})\cdot\vec{\nabla}_2u(r_{23})$$
$$\times[1+h(r_{12})+h(r_{23})+h(r_{13})+h(r_{12})h(r_{23})+h(r_{13})h(r_{23})$$
$$+h(r_{12})h(r_{13})+\rho\int d^3r_4h(r_{14})h(r_{24})h(r_{34})]$$
$$+\rho^2\int d^3r_{12}\int d^3r_{23}\frac{\hbar^2}{8m}\vec{\nabla}_2u(r_{12})\cdot\vec{\nabla}_2u(r_{23})g_3^{\mathrm{RES}}(\vec{r}_{12},\vec{r}_{23})\ . \tag{18}$$

After taking Fourier transforms and performing a little straightforward algebra the following expressions result:

$$T_2=\frac{\hbar^2}{8m}\rho\frac{1}{(2\pi)^3}\int d^3kk^2\tilde{u}(k)^2+\frac{\hbar^2}{8m}\frac{1}{(2\pi)^3}\int d^3k[S(k)-1]\int dp\int dqc_{pq}^k\tilde{u}(p)\tilde{u}(q)\ , \tag{19}$$

$$T_3^{\mathrm{CA}}=\frac{\hbar^2}{8m}\rho\frac{1}{(2\pi)^3}\int d^3kk^2\tilde{u}(k)^2[S(k)-1]$$
$$+\frac{\hbar^2}{8m}\frac{1}{(2\pi)^3}\int d^3k[S(k)-1]\int dp\int dqc_{pq}^k\tilde{u}(p)\tilde{u}(q)[S(p)S(q)-1]\ , \tag{20}$$

$$T_3^{\mathrm{RES}}=\frac{\hbar^2}{8m}\rho\frac{1}{(2\pi)^3}\int d^3k[S(k)-1]k^2R(k)^2 \tag{21a}$$
$$+2\frac{\hbar^2}{8m}\frac{1}{(2\pi)^3}\int d^3k[S(k)-1]\int dp\int dqc_{pq}^k[S(p)-1]R(p)[S(q)-1]\tilde{u}(q) \tag{21b}$$
$$+\frac{\hbar^2}{8m}\frac{1}{(2\pi)^3}\int d^3k[S(k)-1]\int dp\int dqc_{pq}^k[S(p)-1]R(p)[S(q)-1]R(q) \tag{21c}$$
$$+\cdots=T_3^{(3)}+T_3^{(4)}+T_3^{(5)}\ , \tag{21d}$$

with

$$R(k)=\frac{1}{8\rho\pi^2}\frac{1}{k^3}\int dp\int dqpq(k^2+p^2-q^2)$$
$$\times\tilde{u}(p)[S(q)-1]\ , \tag{22}$$

$$c_{pq}^k=(pq/8k\pi^2)(p^2+q^2-k^2)\ , \tag{23}$$

and integrations over p,q are over those regions where

$$|p-q|\leq k\leq p+q\ .$$

While Eqs. (20) to (23) still are exact, because of the terms represented by "$\cdots$," we now have to introduce an approximation in order to actually evaluate T_3. The various terms of Eq. (15) are diagrammatically represented in Fig. 1. As said above, diagrams Figs. 1(a), 1(b), and 1(d) constitute T_3^{CA}. The analytical expression for Fig. 1(c) is given in Eq. (21), term (21a), diagrams Figs. 1(e1) and 1(e2) in term (21b) and Fig. 1(f1) in term (21c). All other diagrams contained in T_3 are distinguished from those represented in Eq. (21) by being *more highly connected*. Consider, for example, Fig. 1(e3). All four points are tied together by either ∇u or a correlation line h. Opposedly in, e.g., Fig. 1(e2) the left and right points may be integrated over independently. In other words, the terms explicitly retained in Eq. (21) are those involving convolution type integrations only, and all other terms involve more highly connected integrations. This argument is made possible by considering the special nature of the three-body operator we are interested in here, last term of Eq. (9). A differentiated correlation line exists between points (1,2) and (2,3) but not between (1,3). The decomposition of g_3 specified in Eqs. (20)–(23) takes account of this special nature in retaining just those terms which are of the hypernetted-chain type omitting those of HNC/4 or /5 type, i.e., having a structure like elementary diagrams. In this sense the approximation suggested here for g_3 is consistent with the hypernetted-chain approximation used for the two-body radial distribution function, Eq. (11), with $E(r)=0$. The argument why this should be a reasonable approximation is just the same as in justifying the hypernetted-chain approximation. In the more highly connected di-

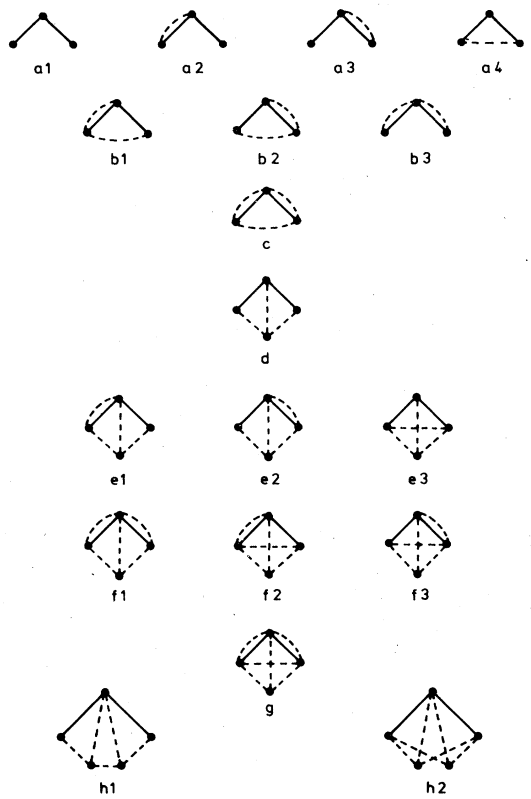

FIG. 1. Diagrammatic representation of the series expansion for the three-body distribution function, Eq. (15), for the special case of the three-body kinetic energy term. Solid lines denote $\vec{\nabla}u(r)$ and dashed lines correlation factors $h(r)$. Solid dots denote coordinates 1, 2, 3 to be integrated over.

agrams of elementary type integration variables are tied to each other making the total volume of integration smaller than for diagrams not being so highly connected. Because of the smaller integration volume, the numerical values for these diagrams should be small and it is justified to neglect them.

Instead of stopping at the four-point level, i.e., including only diagrams Figs. 1(a)–1(d), 1(e1), 1(e2), and 1(f1) as done here, it should be possible to sum *all* diagrams of HNC type including, e.g., Fig. 1(h1) by solving a modified HNC equation. In view of the quantitative results (Sec. III A) this has not been thought worthwhile.

Up to now we considered the simplified Bose wave function Eq. (10). In order to evaluate the expectation value (2) we need to treat the determinantal part of the wave function (1). It is now crucial to notice that we wrote the energy expectation value, Eqs. (7) and (9) in such a way that there occurs no explicit reference to this determinantal part except in the trivial term T_ϕ. The determinant is wholly buried inside the distribution functions g and g_3, which depend only on $|\phi|^2$, see Eqs. (4) and (8). This observation, together with the non-negativity of $|\phi|^2$, enables us to expand rigorously

$$0 \leq \sum_{\sigma_i} |\phi(\vec{r}_1, \ldots, \vec{r}_N)|^2$$

$$= \prod_{i<j} \varphi^2(r_{ij}) \prod_{i<j<k} \varphi_3^2(\vec{r}_i, \vec{r}_j, \vec{r}_k) \prod \varphi_4 \cdots \quad . \tag{24}$$

As an approximation only the first term of this product is retained while all others are neglected. At first sight this might seem to be a very drastic manipulation. However, on the two-body level this approxiation can be made to yield the exact result in the sense that $\varphi(r)$ can be chosen in such a way as to reproduce the exact two-body radial distribution function $g_F(r)$ corresponding to the full determinant. Explicitly, denoting by g_F and S_F the distribution function and structure factor corresponding to a purely determinantal wave function, $\varphi(r)$ may be obtained from

$$\varphi(r) = \exp[\tfrac{1}{2} w(r)] \ ,$$

$$w(r) = \ln g_F(r) - \frac{1}{\rho} \left[\frac{[S_F(k)-1]^2}{S_F(k)} \right]^F \ . \tag{25}$$

Then, by construction, cf. Eq. (11), if this $\varphi(r)$ is used in a hypernetted-chain evaluation of g_F, the exact result is obtained. Of course differences will arise on the three-body level. Note that, since

$$S_F(k) = \begin{cases} \frac{3}{4} k/k_F - \frac{1}{16} (k/k_F)^3, & k \leq 2k_F \\ 1, & k \geq 2k_F, \end{cases}$$

$\tilde{w}(k) \sim k^{-1}$ for small k, i.e., $w(r)$ is a long-ranged function.

The essence of this procedure to treat the determinantal part of the wave function has been suggested by Lado[16] and was refined[17] and used[18] by Stevens and Pokrant in a calculation on the electron fluid. One might ask why we prefer to use this method to treat antisymmetry rather than one of the more widely used methods[13,15] of expansion in permutations. The latter method, which has been used by Lantto and Siemens in their calculation on the electron fluid,[2] suffers from an inaccurate treatment of long-range exchange effects as was pointed out by Krotscheck.[7] Since such long-range effects *a priori* should be important in the case of the electron fluid—while their importance is questionable for short-range forces[12,13] —a method circumventing this problem is preferable.

The truncation of the product (24) may further be justified using diagrammatic methods.[13] In the language of the permutation expansion, in the long-

range (long-wavelength) limit certain elementary diagrams which are omitted in a HNC treatment become as large as some of the diagrams included in the HNC summation. In the present treatment, these elementary diagrams are approximated consistently through all orders.[13]

The present method has the additional advantage that the fermion problem is completely reduced to an equivalent Bose problem. For fermions, from Eqs. (11) and (25) the connection between radial distribution function and wave function is given in HNC approximation by

$$u(r)=\ln g(r)-\frac{1}{\rho}\left[\frac{[S(k)-1]^2}{S(k)}\right]^F-w(r) \quad . \tag{26}$$

The preceding equation follows immediately from Eq. (11) if one writes the square of the wave function (1) as

$$\begin{aligned}&|\psi(\vec{r}_1,\ldots,\vec{r}_N)|^2=\prod_{i<j}\hat{f}^2(r_{ij}) \quad ,\\ &\hat{f}(r)=\exp[\tfrac{1}{2}u(r)+\tfrac{1}{2}w(r)]=f(r)\varphi(r) \quad .\end{aligned} \tag{27}$$

In other words, the Fermi-HNC equation is one nonlinear integral equation as in the Bose case, as opposed to several coupled equations obtained in the permutation expansion approach.[2,3,13,15] Even more significant, the representation of the three-body radial distribution function g_3 in terms of $g(r)-1$, Eq. (15) and Fig. 1, remains unaffected by Fermi statistics as opposed to enormous complications in the permutation-expansion scheme.[12,13]

A further important observation is that for arbitrary, short-range correlation factors $f(r)$ where $\tilde{u}(k)$ is bounded for $k\to 0$ it follows immediately from Eq. (26) that $S(k)\to S_F(k)$ for $k\to 0$ since $\tilde{w}(k)\sim S_F(k)^{-1}$ and all other terms are bounded. This behavior is opposed to that of the Fermi-HNC equations as derived by Fantoni and Rosati[3] and used by Lantto and Siemens[2] where $S(k)$ does not necessarily go to zero for small k for arbitrary correlation factors. If the pseudopotential $\tilde{u}(k)$ diverges like k^{-1} at the origin it is seen that the slope of $S(k)$ at the origin will be modified but $S(k)$ will remain linear. Only if $\tilde{u}(k)$ diverges like k^{-2} at the origin will $S(k)$ become quadratic in k.

To summarize the present section, an energy expression is obtained from Eqs. (7) and (18)–(23) involving only the "pseudopotential" u and the structure factor $S(k)$. One of these two functions is determined by the other using the HNC equation (26)

$$\tilde{u}(k)=\left[\ln\left[\frac{1}{\rho}[S(k)-1]^F+1\right]\right]^F-\frac{1}{\rho}\frac{[S(k)-1]^2}{S(k)}-\tilde{w}(k) \quad , \tag{28}$$

where w is known from Eq. (25). A second equation determining the second unknown function will be derived in the next section.

B. Wave-function optimization

I wish to determine the optimal wave function of the form (1). The determinant is assumed to be known, i.e., a filled Fermi sphere of appropriate radius k_f, determined from density and polarization. I wish to minimize the variational energy functionally, Eq. (2), with respect to the correlation factor $f(r)$, Eq. (1), or equivalently the pseudopotential u, Eq. (12)

$$\frac{\delta}{\delta u}\frac{\langle\psi|H|\psi\rangle}{\langle\psi|\psi\rangle}=\frac{\delta}{\delta u}E[u,S]=0 \quad , \tag{29}$$

subject to the HNC equation as a constraint

$$S=S[u] \quad .$$

Since the HNC equation (28) is an explicit equation for u, it is most convenient to eliminate the pseudopotential u everywhere by expressing it in terms of the structure factor $S(k)$. A single nonlinear integral equation for the one unknown function $S(k)$ is obtained

$$\frac{\delta}{\delta S}E[u[S],s]=0 \quad . \tag{30}$$

Neglecting for the moment the term T_3^{RES} this equation is explicitly

$$\begin{aligned}&\frac{1}{4\pi^2}k^2\tilde{v}(k)+\frac{\hbar^2}{16m\pi^2}\rho k^4\tilde{u}^2(k)+\frac{\hbar^2}{16m\pi^2}2\rho\int dl l^4S(l)\tilde{u}(l)D_{lk}+\frac{\hbar^2}{16m\pi^2}k^2\int dp\int dq c^k_{pq}\tilde{u}(p)S(p)\tilde{u}(q)S(q)\\ &\quad+\frac{\hbar^2}{16m\pi^2}2\int l^2dl[S(l)-1]\int dp\int dq c^l_{pq}\tilde{u}(p)S(p)[D_{qk}S(q)+\tilde{u}(q)\delta_{qk}]=0 \quad ,\end{aligned} \tag{31}$$

where u is given in terms of S by Eq. (28),

$$D_{lk}=\frac{\delta\tilde{u}(l)}{\delta S(k)}=\frac{\delta_{lk}}{\rho S^2(k)}+\frac{2k^2}{\rho\pi}\int drr^2j_0(lr)j_0(kr)\left[\frac{1}{g(r)}-1\right]=\frac{\delta_{lk}}{\rho S^2(k)}-\frac{1}{4\rho\pi^2}\int_{|l-k|}^{l+k}dq\frac{kq}{l}\left[\frac{1}{g(r)}-1\right]^F(q) \quad , \tag{32}$$

and $g(r)$ is given in terms of S by Eq. (6). Since everything is expressed in terms of the structure factor $S(k)$ Eq. (31) may be solved to yield the $S(k)$ corresponding to the optimal Jastrow wave function (1). The wave function itself, i.e., the pseudopotential u may then be obtained from Eq. (28), and the approximation to a least upper bound to the ground-state energy from Eqs. (7) and (18) to (23).

It is to be noted that for zero potential, i.e., in the noninteracting case, Eq. (31) becomes homogeneous in u and therefore has $u \equiv 0$ as a solution. Considering Eqs. (25) and (26) it follows that the correct result, $S = S_F$, $g = g_F$ obtains. In other words, the Euler-Lagrange equation (31) is correct for arbitrarily weak interactions which is a necessary condition in order to deal with the high-density limit for the electron fluid, and which is not true of certain other approaches.[13]

Before attempting to solve Eq. (31) numerically let us study the properties of its solutions by considering the small k, i.e., long-wavelength, limit of this equation. We are interested in solutions $S(k)$ proportional to k^2 for small k. In that case, from Eq. (28) we have

$$\tilde{u}(k) = -\frac{1}{\rho S(k)} + \frac{1}{\rho S_F(k)} \tag{33}$$

since from Eq. (25)

$$\tilde{w}(k) = -\frac{1}{\rho S_F(k)} \ . \tag{34}$$

Because $g(r)$ will remain positive for small r in the second term of Eq. (32) we may approximate for the long-range part $g^{-1}(r) - 1 \approx 1 - g(r)$ and obtain

$$D_{lk} \approx \frac{\delta_{lk}}{\rho S^2(k)} - \frac{1}{4\rho^2\pi^2} \int_{|l-k|}^{l+k} dq \frac{kq}{l} [S(q) - 1] \ ,$$

which for small k becomes

$$D_{lk} = \frac{\delta_{lk}}{\rho S^2(k)} - \frac{1}{2\rho^2\pi^2} k^2 [S(l) - 1] \ .$$

Collecting all this together, Eq. (31) becomes, retaining for all terms only the leading contribution,

$$\frac{1}{4\pi^2} k^2 \frac{4\pi e^2}{k^2} + \frac{\hbar^2}{16m\pi^2} \frac{1}{\rho} k^4 \left(\frac{1}{S_F(k)} - \frac{1}{S(k)} \right)^2 \tag{35a}$$

$$+ \frac{\hbar^2}{16m\pi^2} \frac{2}{\rho} k^4 \frac{1}{S(k)} \left(\frac{1}{S_F(k)} - \frac{1}{S(k)} \right) \tag{35b}$$

$$- \frac{\hbar^2}{16m\pi^2} k^2 \frac{1}{\rho\pi^2} \int dl l^4 S(l)[S(l) - 1]\tilde{u}(l) \tag{35c}$$

$$+ \frac{\hbar^2}{16m\pi^2} k^2 \frac{1}{2\pi^2} \int dp p^4 S^2(p)\tilde{u}^2(p) \tag{35d}$$

$$+ \frac{\hbar^2}{16m\pi^2} k^4 \frac{2}{\rho} \frac{1}{S_F(k)} \frac{1}{4\pi^2} \int dl l^2 \tilde{u}(l) S(l)[S(l) - 1] \tag{35e}$$

$$- \frac{\hbar^2}{16m\pi^2} k^2 \frac{1}{\rho^2\pi^2} \int dl l^2 [S(l) - 1] \int dp \int dq c_{pq}^{l} \tilde{u}(p) S(p) S(q)[S(q) - 1] = 0 \ . \tag{35f}$$

Here, the Coulomb potential has been inserted explicitly. In the last two terms of Eq. (31) the expression (23) for the c coefficients has been used to find the small-k behavior of the integrals. It is seen that in this limit only the first three terms of Eq. (31) need to be retained, Eqs. (35a) and (35b), since the remaining two vanish. The resulting simple quadratic equation for $S(k)$ may easily be solved to yield

$$S(k) = k^2(\hbar^2/16m\pi\rho e^2)^{1/2} = k^2/2m\omega_p \ , \tag{36}$$

with ω_p the plasma frequency which is known to be the exact behavior.[19] The same behavior has been found by Lantto and Siemens[2] and is also found in the case of charged bosons. A difference should arise in the next term of a power-series expansion of $S(k)$ where the fermion character of the wave function in form of S_F factors will first enter. Unfortunately it seems to be hard to obtain the next term, since nonleading contributions to some of the terms of Eq. (31) are required.

In the above discussion, the term T_3^{RES} was neglected. The approximation used so far for the three-body distribution function has been the convolution form, satisfying the sequential relation, Eq. (16). T_3^{RES} as given in Eq. (21) expresses the leading terms going beyond this approximation. However, these terms do not integrate to zero as is necessary to preserve Eq. (16). In other words, in the volume integral these terms should not contribute at all.

It is rather straightforward to include the terms given explicitly in Eq. (21) into the Euler equation (31). However doing so leads to a modification of the low-momenum behavior Eq. (36) since

$$\frac{\delta T_3^{\mathrm{RES}}(a)}{\delta S(k)} \to k^2 c_1 + \frac{k^4}{S^2(k)} c_2 \ ,$$

$$\frac{\delta T_3^{\mathrm{RES}}(b)}{\delta S(k)} \to k^2 c_3 + \frac{k^4}{S^2(k)} c_4 \ ,$$

$$\frac{\delta T_3^{\mathrm{RES}}(c)}{\delta S(k)} \to k^2 c_5 + \frac{k^4}{S^2(k)} c_6 \ ,$$

$$c_1 = \frac{\hbar^2}{16 m \pi^4} \int dq q^4 [S(q)-1] R(q) \tilde{u}(q) \ ,$$

$$c_2 = \frac{\hbar^2}{32 m \pi^4 \rho} \int dq q^2 [S(q)-1]^2 R(q) \ , \tag{37}$$

$$c_3 = \frac{\hbar^2}{16 m \pi^4} \int dp p^4 [S(p)-1]^2 \tilde{u}(p) R(p) + \frac{\hbar^2}{16 m \pi^4 \rho} \int l^2 dl [S(l)-1] \int dp \int dq c_{pq}^l [S(p)-1] \tilde{u}(p) [S(q)-1] \tilde{u}(q) \ ,$$

$$c_4 = \frac{-\hbar^2}{32 m \pi^4 \rho} \int l^2 dl [S(l)-1]^2 R(l) + \frac{\hbar^2}{32 m \pi^4 \rho^2} \int l^2 dl [S(l)-1] \int dp \int dq c_{pq}^l [S(p)-1] \tilde{u}(p) [S(q)-1]^2 q^{-2} \ ,$$

$$c_5 = \frac{\hbar^2}{32 m \pi^4} \int dp p^4 [S(p)-1]^2 R^2(p) + \frac{\hbar^2}{16 m \pi^2 \rho} \int l^2 dl [S(l)-1] \int dp \int dq c_{pq}^l [S(p)-1] R(p) [S(q)-1] \tilde{u}(q) \ ,$$

$$c_6 = \frac{\hbar^2}{32 m \pi^4 \rho^2} \int l^2 dl [S(l)-1] \int dp \int dq c_{pq}^l [S(p)-1] R(p) [S(q)-1]^2 q^{-2} \ ,$$

in the $k \to 0$ limit. There is significant cancellation between c_2, c_4, and c_6 but they do not cancel completely.

Though this modification might be expected to be small in most instances it does lead to a wrong coefficient in Eq. (36). Even more serious, the argument of the square root in Eq. (36) cannot be guaranteed to be positive any more. In other words there does not necessarily exist a solution to the Euler-Lagrange equation any more, or, the energy may become unbounded from below. Similar observations, using the superposition form for the three-body distribution function, have been made previously.[20] The nonexistence of solutions is related to a negative kinetic energy expectation value and correspondingly unphysical distribution functions $g(r)$ for which the HNC approximation is not valid. On the other hand, if one computes the optimal wave function from Eq. (31) as it stands and then evaluates T_3^{RES} as a correction extremely small values are found (see Sec. III) as is appropriate for a high-order correction term. These findings underline the paramount importance of the sequential relation [Eq. (16)] in optimizing the wave function. I will therefore proceed using only the convolution form for g_3, and use the higher-order contributions as perturbative corrections to the energy only.

In order to sovle Eq. (31) numerically, the Newton-Raphson iteration scheme is used. After discretization of the integrals a system of nonlinear coupled algebraic equations obtains

$$\frac{d}{dS(k_i)} E[S(k_j)] = 0 \ . \tag{38}$$

Because of the triangular property of the c coefficients it has been found expedient to use equidistant mesh points. Assuming a current iterate $S_k^{[\nu]}$, Eq. (38) is linearized at this vector, and the resulting linear system of equations is solved to produce a new iterate $S_k^{[\nu+1]}$.

$$S_k^{[\nu+1]} = S_k^{[\nu]} - \left[\frac{d^2 E[S_k^{[\nu]}]}{dS_i dS_k} \right]^{-1} \frac{dE[S_k^{[\nu]}]}{dS_i} \ . \tag{39}$$

Since the analytically known matrix $d^2E/dS_i dS_k$ is obtained in this process anyway, it is easy to verify numerically

$$\frac{\delta^2 E}{\delta S_i \delta S_k} > 0$$

in the sense that all eigenvalues are positive. We are therefore assured to have found a true minimum of the energy functional (30).

All the equations in this section have carefully

been written in momentum space such that the singularities at the origin are clearly exhibited. In this form these equations are immediately suitable for numerical treatment. The only exception where a coordinate-space quantity must be used is the second term of Eq. (32). One could avoid coordinate space at the expense of solving a linear system of equations in momentum space (equivalent to the inversion in coordinate space) but I prefer to evaluate $g(r)$ by Fourier transform, compute the integrand in Eq. (32), and perform the integration, which does not pose any particular difficulty. It is necessary, however, to restrict the first few steps of the iteration (39) to such $S(k)$ that $S(k)$ and $g(r)$ remain positive.

C. Mean spherical approximation

In order to study further the properties of Eq. (31) let me consider the limit of high densities, i.e., small values of the customary parameter r_s

$$\rho = (\tfrac{4}{3}\pi r_s^3 a_0^3)^{-1} , \tag{40}$$

which is the average interparticle spacing in units of the Bohr radius a_0. In this case it is known[19] that only long-range effects matter where $g(r)$ is close to one. The logarithm in Eq. (26) may then be replaced by its argument minus one to obtain

$$\tilde{u}(k) = \frac{1}{\rho}[S(k)-1] - \frac{1}{\rho}\frac{[S(k)-1]^2}{S(k)} - \tilde{w}(k)$$
$$= \frac{1}{\rho}\left[1 - \frac{1}{S(k)}\right] - \tilde{w}(k) . \tag{41}$$

This equation has been used previously in the theory of classical liquids[21] and been given the name mean spherical approximation (MSA). It is closely related to Feenberg's uniform limit.[10] Equation (32) becomes

$$D_{lk} = \frac{\delta\tilde{u}(l)}{\delta S(k)} = \frac{\delta_{lk}}{\rho S^2(k)} .$$

For consistency, we also have to modify Eq. (25) in the same way to obtain

$$\tilde{w}(k) = \frac{1}{\rho}\left[1 - \frac{1}{S_F(k)}\right] \tag{42}$$

and together with Eq. (41)

$$\tilde{u}(k) = \frac{1}{\rho}\left[\frac{1}{S_F(k)} - \frac{1}{S(k)}\right] .$$

Furthermore, since we did not find any contributions from the last two terms of Eq. (31) in the long-wavelength limit, these terms are neglected. The Euler-Lagrange equation now reads

$$\frac{1}{4\pi^2}k^2\frac{4\pi e^2}{k^2} + \frac{\hbar^2}{16m\pi^2}\rho k^4\frac{1}{\rho^2}\left[\frac{1}{S_F(k)} - \frac{1}{S(k)}\right]^2 + \frac{\hbar^2}{16m\pi^2}2\rho k^4 S(k)\frac{1}{\rho}\left[\frac{1}{S_F(k)} - \frac{1}{S(k)}\right]\frac{1}{\rho}\frac{1}{S^2(k)} = 0 \tag{43}$$

with the immediate solution

$$S^{\mathrm{MSA}}(k) = k^2\left[\frac{\hbar^2}{16m\pi e^2\rho}\right]^{1/2}\left[1 + \frac{\hbar^2}{16m\pi e^2\rho}k^4\frac{1}{S_F^2(k)}\right]^{-1/2} \tag{44}$$

From this result one easily obtains the pseudopotential u and the energy from Eqs. (7), (19), and (20) which read after some algebraic manipulation

$$\epsilon_c = -\left[\frac{9\pi}{4}\right]^{5/3}\Big/(6\pi r_s^2)\int_0^\infty \frac{dq}{S_F(q)}\left\{q^2 - \left[12\left[\frac{9\pi}{4}\right]^{-4/3} r_s S_F^2(q) + q^4\right]^{1/2}\right\}^2 , \tag{45}$$

when q is in units k_F now and energies are measured in Rydberg. In the limit $r_s \to 0$ this integral may be evaluated in closed form[22] to yield, for the spin unpolarized system

$$\epsilon_c \to (9/16\pi^2)\ln r_s \approx 0.056\,99 \ln r_s \text{ Ry} . \tag{46}$$

The correlation energy ϵ_c is defined as the difference between the total energy per particle and the Hartree-Fock value

$$\epsilon_{\mathrm{HF}} = T_\phi + V_{\mathrm{HF}}$$
$$= T_\phi + \frac{1}{2(2\pi)^3}\int d^3k \frac{4\pi e^2}{k^2}[S_F(k)-1] . \tag{47}$$

The correlation energy [Eq. (46)] is to be compared with the known exact result in the high-density limit[19,23]

$$\epsilon_c \to (2/\pi^2)(1-\ln 2)\ln r_s \approx 0.062\,18 \ln r_s \text{ Ry} . \tag{48}$$

The 8.4% difference between Eqs. (46) and (48) is known to arise from the use of state-independent correlation factors in the variational wave function (1).[24] The behavior of Eq. (46) may also be obtained from the random-phase approximation (RPA) if one introduces the assumption of state independence there.[4] It is a straightforward but lengthy calculation to show that the result [Eq. (46)] also obtains directly

from Eq. (31) in the high-density limit. The difference between Eqs. (46) and (48) is thought to be totally irrelevant for $r_s > 2$ since the series expansion of Ref. 19 requires $r_s \ll 1$.

D. Model energies

In nonvariational theories one frequently calculates the energy from the unsymmetrical expression

$$E_{\text{mod}} = \frac{1}{N}\frac{\langle\phi|H|\psi\rangle}{\langle\phi|\psi\rangle} \quad , \tag{49}$$

which is called a "model energy" since for any ψ that is not a solution of Schrödinger's equation its value will depend on the "model" wave function ϕ chosen, which usually is a plane-wave determinant. The deviation of Eq. (49) from the exact Schrödinger eigenvalue is proportional to the error in the wave function, whereas it is quadratic in the error in the wave function for the variational energy [Eq. (2)]. Therefore, the difference between variational and model energy constitutes some measure of the "distance" between the variational wave function and the true ground-state wave function.[12,13,25]

The model energy has a kinetic and a potential energy contribution

$$E_{\text{mod}} = \frac{1}{N}\frac{\langle\phi|T|\psi\rangle}{\langle\phi|\psi\rangle} + \frac{1}{N}\frac{\langle\phi|V|\psi\rangle}{\langle\phi|\psi\rangle}$$
$$= T_\phi + \frac{1}{2(2\pi)^3}\int d^3k \frac{4\pi e^2}{k^2}[S_\phi(k)-1] \quad , \tag{50a}$$

$$\epsilon_c^{\text{mod}} = \int dk \frac{e^2}{\pi}[S_\phi(k) - S_F(k)] = \int dk\, \epsilon_\phi(k) \quad , \tag{50b}$$

where we use the fact that ϕ is an eigenfunction of T and $S_\phi(k)$ is defined by

$$S_\phi(k) = \frac{1}{N}\frac{\langle\phi|\rho_{\vec{k}}\rho_{-\vec{k}}F|\phi\rangle}{\langle\phi|F|\phi\rangle}$$
$$= \frac{1}{N}\frac{\langle\phi|\sqrt{F}\,\rho_{\vec{k}}\rho_{-\vec{k}}\sqrt{F}\,|\phi\rangle}{\langle\phi|\sqrt{F}\sqrt{F}\,|\phi\rangle} \quad . \tag{51}$$

The last equality in Eq. (51) holds since the operators F and

$$\rho_{\vec{k}}\rho_{-\vec{k}} = \left[\sum_{i=1}^{N} e^{i\vec{k}\cdot\vec{r}_i}\right]\left[\sum_{i=1}^{N} e^{-i\vec{k}\cdot\vec{r}_i}\right]$$

are local and therefore commute. Another way to express the usual structure factor is[10]

$$S(k) = \frac{1}{N}\frac{\langle\psi|\rho_{\vec{k}}\rho_{-\vec{k}}|\psi\rangle}{\langle\psi|\psi\rangle} \quad . \tag{52}$$

The analogy to Eq. (51) is obvious. It is only necessary to replace the correlation factor by its square root in order to obtain the "model structure factor" S_ϕ, in HNC approximation

$$\tfrac{1}{2}\tilde{u}(k) = \left[\ln\left[\frac{1}{\rho}[S_\phi(k)-1]^F + 1\right]\right]^F$$
$$- \frac{1}{\rho}\frac{[S_\phi(k)-1]^2}{S_\phi(k)} - \tilde{w}(k) \quad . \tag{53}$$

Equation (53) is an implicit equation for $S_\phi(k)$ where the pseudopotential u is known from the solution of the Euler-Lagrange equation. This equation may readily be solved by the same techniques used to solve Eq. (31).

The model structure factor is a very useful quantity for comparisons with other theories of the electron fluid. The most advanced treatment in terms of partially summed perturbation series is given by Bishop and Lührmann.[4,23] They focus on the two-particle two-hole excitation amplitude

$$\langle\vec{k}_1+\vec{q}\sigma_1\vec{k}_2-\vec{q}\sigma_2|S_2|\vec{k}_1\sigma_1\vec{k}_2\sigma_2\rangle = \langle\phi|a^\dagger_{\vec{k}_1\sigma_1}a^\dagger_{\vec{k}_2\sigma_2}a_{\vec{k}_2-\vec{q}\sigma_2}a_{\vec{k}_1+\vec{q}\sigma_1}|\psi\rangle/\langle\phi|\psi\rangle$$
$$- \langle\phi|a^\dagger_{\vec{k}_1\sigma_1}a^\dagger_{\vec{k}_2\sigma_2}a_{\vec{k}_2-\vec{q}\sigma_2}a_{\vec{k}_1+\vec{q}\sigma_1}|\phi\rangle \quad . \tag{54}$$

Because of the operator identity

$$\rho_{\vec{q}} = \sum_{\vec{k}\sigma} a^\dagger_{\vec{k}\sigma}a_{\vec{k}+\vec{q}\sigma} \tag{55}$$

we have[26]

$$\sum_{\vec{k}_1\sigma_1,\,\vec{k}_2\sigma_2}^{k_F} \langle\vec{k}_1+\vec{q}\sigma_1\vec{k}_2-\vec{q}\sigma_2|S_2|\vec{k}_1\sigma_1\vec{k}_2\sigma_2\rangle$$
$$= N[S_\phi(q)-S_F(q)] = \frac{N\pi}{e^2}\epsilon_\phi(q) \quad . \tag{56}$$

The last equality indicates the immediate connection to the correlation energy, Eq. (50b). The average over the Fermi sphere performed in Eq. (56) is just the one necessary to obtain the correlation energy from S_2 [see Eq. (50b)]. It is therefore possible to compare the *integrands* of Eq. (50b) obtained from different theories. This comparison is much more meaningful than the comparison of structure factors or distribution functions since it may be seen how different momentum transfers k contribute to the correlation energy.

From the RPA it is known[23] that the integrand $\epsilon_\phi(k)$ of Eq. (50b) behaves like

$$\epsilon_\phi^{\mathrm{RPA}}(q) \overset{q\to\infty}{\longrightarrow} \frac{-8}{3\pi^2} q^{-4} \ , \qquad \epsilon_\phi^{\mathrm{RPA}}(q) \overset{q\to 0}{\longrightarrow} \frac{-3}{2\pi}\left(\frac{4}{9\pi}\right)^{-1/3} \frac{q}{r_s} \ , \tag{57}$$

where q again is dimensionless and energies are in Ry. Since the RPA is a high-density approximation, it is appropriate to compare with the corresponding limit of the variational theory, the MSA. Here we have, from Eqs. (41) through (45)

$$\tilde{u}(k) = \rho^{-1}[S_F^{-1}(k) - S^{-1}(k)] \ , \tag{58a}$$

$$\tfrac{1}{2}\tilde{u}(k) = \rho^{-1}[S_F^{-1}(k) - S_\phi^{-1}(k)] \ , \tag{58b}$$

$$S_\phi^{\mathrm{MSA}}(k) = \frac{2S_F(k)}{1+\{(16\pi e^2 m\rho/\hbar^2)[S_F^2(k)/k^4]+1\}^{1/2}} \ , \tag{58c}$$

$$\epsilon_\phi^{\mathrm{MSA}}(q) = -(\tfrac{1}{4}9\pi)^{5/3}/(6\pi r_s^2) S_F^{-1}(q) \times \{q^2 - [12(\tfrac{1}{4}9\pi)^{-4/3} r_s S_F^2(q) + q^4]^{1/2}\}^2 \ . \tag{58d}$$

First note that the integrand for the model energy, Eq. (58d), is the same as for the variational energy, Eq. (45). Therefore, model and variational energies are identical for the MSA for any density. Furthermore, taking the appropriate limits, Eq. (58d) reproduces Eq. (57). We conclude that the RPA is contained in our variational theory as the high-density limit with the reservation about state dependence made above. A more detailed and quantitative comparison of perturbational and variational results will be performed in Sec. III B.

E. Low-density limit

It is well known that in the limit of low density the electron fluid may be considered to be a system of interacting bosons, or Boltzmann particles, since statistics do not matter at all in this limit. The Bose limit of any equation in this paper is easily obtained by setting $S_F = 1$, corresponding to $\phi = 1$. In this case various partial integrations may be performed in the kinetic energy expectation value. An especially useful rigorous formula for the kinetic energy is the Jackson-Feenberg (JF) form[12,13,15,27]

$$T_{\mathrm{JF}} = T_\phi + \frac{\hbar^2}{16m\pi^2}\int dk k^4 [S(k)-1]\tilde{u}(k) \ , \tag{59}$$

$$T_\phi = 0 \ ,$$

from which we immediately have the Euler-Lagrange equation

$$\frac{1}{4\pi^2}k^2\tilde{v}(k) + \frac{\hbar^2}{16m\pi^2}k^4\tilde{u}(k) + \frac{\hbar^2}{16m\pi^2}\int dp p^4 [S(p)-1]D_{pk} = 0 \ . \tag{60}$$

The important feature of this form for bosons is that the three-body distribution function g_3 is not required. By comparing the results of Eqs. (60) and (31) for bosons it is therefore possible to estimate the convergence of the series expansion for g_3 [Eq. (15)] used in the present paper. Unfortunately for fermions it is not possible to use the JF form in the present context since derivatives of the determinant would be involved which cannot be accommodated within the scheme of Eqs. (24) and (25).

The low momentum limit of Eq. (60) is

$$\frac{1}{4\pi^2}k^2\frac{4\pi e^2}{k^2} - \frac{\hbar^2}{16m\pi^2}\frac{k^4}{\rho S(k)} - \frac{\hbar^2}{16m\pi^2}\frac{k^4}{\rho S^2(k)} - \frac{\hbar^2}{16m\pi^2}\frac{k^2}{2\rho^2\pi^2}\int dp p^4 [S(p)-1]^2 = 0 \ . \tag{61}$$

It is trivial to see that the solution $S(k)$ will have the correct behavior for small k, Eq. (36), since the second and the last term vanish. A similar result has been obtained in Ref. 28.

F. Short-range limit

In the limit of small pair distances, $r_{ij} \to 0$, the Euler-Lagrange equation (31) considerably simplifies since only two-particle processes matter. Three- and many-body contributions may be neglected. The energy expression used in this paper, Eqs. (5) and (18), simplifies to

$$\frac{\langle H\rangle}{N} = T_\phi + \rho\int d^3 r g(r)\frac{\hbar^2}{8m}[\nabla u(r)]^2 + \tfrac{1}{2}\rho\int d^3 r v(r)[g(r)-1]$$

yielding upon functional variation with respect to $u(r)$ the short-range Euler-Lagrange equation

$$\frac{e^2}{r} - \frac{\hbar^2}{m}\frac{1}{r}u'(r) = 0$$

with the immediate solution

$$u'(0) = e^2 m/\hbar^2 = a_0^{-1} \ .$$

This is the well-known cusp condition.[1] Since all approximations involved in the solution of the full Eq. (31) affect only three- and more-particle contribu-

tions, the solutions obtained will in principle satisfy the cusp condition exactly. However, since numerically I choose to solve Eq. (31) in momentum space on a finite interval of momenta, at very small distances corresponding to infinite momentum contributions the Euler-Lagrange equation will not be satisfied. In fact, for any function $\tilde{f}(k)$ defined on a *finite* interval, the slope of the Fourier transform at the origin

$$\lim_{r\to 0}\frac{d}{dr}\frac{4\pi}{(2\pi)^3}\int_0^K k^2 dk\tilde{f}(k)j_0(kr) = \frac{4\pi}{(2\pi)^3}\int_0^K k^3 dk\tilde{f}(k)\lim_{r\to 0} j_1(kr) = 0 \ .$$

In practice, the pseudopotential $u(r)$ does attain the correct slope $1/a_0$ at small but finite values of r but eventually for distances less than K^{-1} corresponding to $k_F r < 0.05$ becomes flat.

III. RESULTS

A. Charged Bose fluid

In order to test first the convergence of the series expansion Eq. (15) for the three-body distribution function let me consider a system of charged bosons having the electron mass immersed in a positive uniform background. The second column of Table I gives the optimal energies per particle as a function of mean interparticle spacing r_s obtained by solving Eq. (60) and calculating the energy from Eqs. (7) and (59); i.e., the Jackson-Feenberg form of the energy is employed. Here, the three-body distribution function does not enter at all. These results are identical to those of Lee and Ree[29] obtained by applying a paired phonon analysis, which is equivalent to an energy minimization in the space of function (1). In the high-density or uniform limit[10] it is easily verified that Eqs. (7), (59), and (60) yield the known exact result

$$\epsilon_c \to -0.8031 r_s^{-3/4} \text{ Ry} \ .$$

Note that for charged bosons correlation energy and total energy are identical since the Hartree term does not exist.

The third column of Table I gives the energies obtained from the Clark-Westhaus form for the kinetic energy and using the convolution form for the three-body distribution function, i.e., solving the Bose version of Eq. (31) and calculating the energy from Eqs. (7) and (18)–(20). The following three columns give the terms of Eq. (21) and the resulting total energy may be found in column 7. Again it is rather easy to show that in the high-density limit the exact result is obtained. At finite densities small differences arise between the different kinetic energy formulas due to the HNC approximation and approximation of g_3. Note first that the CW energies are al-

TABLE I. Energies for the charged Bose fluid. $E_{\text{JF}}^{\text{OPT}}$, from minimizing the Jackson-Feenberg energy functional, Eq. (60); $E_{\text{CW-CA}}^{\text{OPT}}$, from minimizing the Clark-Westhaus energy functional, Eq. (31), and using the convolution approximation for the three-body distribution function, Eq. (20); (21a), (21b), and (21c), terms of Eq. (21) corrections to the kinetic energy expectation value; E, sum of previous four columns; E_{JF}, energy from Jackson-Feenberg functional but using the wave function obtained from the Clark-Westhaus functional; E_{mod}, model energy, Eq. (50), using the wave function obtained from the CW functional; $g(r=0)$, value of the radial distribution function at the origin; E_{MSA}, energy obtained from the mean spherical approximation, Eq. (44). All energies in rydberg units.

r_s	$E_{\text{JF}}^{\text{OPT}}$	$E_{\text{CW-CA}}^{\text{OPT}}$	(a)	(b)	(c)	E	E_{JF}	E_{mod}	$g(r=0)$	E_{MSA}
1	−0.7756	−0.7749	−0.0017	0.0013	−0.0001	−0.7754	−0.7756	−0.7753	0.474	−0.8025
2	−0.4508	−0.4499	−0.0024	0.0019	−0.0001	−0.4505	−0.4508	−0.4498	0.293	−0.4769
3	−0.3263	−0.3252	−0.0027	0.0022	−0.0002	−0.3259	−0.3263	−0.3249	0.198	−0.3517
4	−0.2585	−0.2574	−0.0029	0.0024	−0.0002	−0.2583	−0.2585	−0.2569	0.142	−0.2833
5	−0.2154	−0.2142	−0.0029	0.0026	−0.0003	−0.2149	−0.2153	−0.2137	0.106	−0.2396
8	−0.1456	−0.1445	−0.0029	0.0027	−0.0003	−0.1452	−0.1455	−0.1438	0.055	−0.1682
10	−0.1205	−0.1195	−0.0028	0.0027	−0.0004	−0.1200	−0.1204	−0.1188	0.039	−0.1422
14	−0.0902	−0.0893	−0.0026	0.0026	−0.0004	−0.0897	−0.0900	−0.0887	0.024	−0.1103
16	−0.0804	−0.0794	−0.0025	0.0025	−0.0004	−0.0797	−0.0801	−0.0789	0.020	−0.0998
20	−0.0661	−0.0652	−0.0023	0.0024	−0.0004	−0.0654	−0.0659	−0.0647	0.015	−0.0843
24		−0.0555	−0.0021	0.0023	−0.0004	−0.0557	−0.0560	−0.0550	0.012	−0.0734
28		−0.0483	−0.0020	0.0022	−0.0004	−0.0484	−0.0488	−0.0479	0.010	−0.0654
32		−0.0428	−0.0019	0.0021	−0.0004	−0.0429	−0.0433	−0.0425	0.0085	−0.0591
36		−0.0385	−0.0018	0.0021	−0.0004	−0.0386	−0.0389	−0.0382	0.0074	−0.0540
40		−0.0350	−0.0017	0.0020	−0.0004	−0.0350	−0.0353	−0.0347	0.0065	−0.0499

ways above the JF energies so that we are reassured that the CW form will tend to preserve the upper-bound property of the variational energy. Moreover, the corrections from the series expansion of the three-body distribution function are rather small and tend to cancel each other such that the total correction to the convolution approximation is always less than a millirydberg. In this context it is amusing to note that the contribution due to the Kirkwood superposition form for g_3, term (21a), is almost precisely canceled by term (21b) which in other approaches is part of a HNC/4-type contribution. This clearly points out the inadequacy of the superposition approximation, and illustrates the large positive contributions.[12,13,15] It is clear that using term (21a) alone might easily lead to an energy estimate which is *not* an upper bound to the ground-state energy.

The eighth column of Table I gives an energy evaluated from the wave function obtained in the last paragraph, but using the Jackson-Feenberg from Eq. (59) for the kinetic energy. It is seen that this energy is almost precisely equal to the one obtained by minimizing the Jackson-Feenberg form itself (column 2). This comparison illustrates the similarity of the wave functions obtained in either minimization procedure. Figure 2 shows the structure functions $S(k)$ obtained both ways for $r_s = 20$ which are nearly indistinguishable. For smaller values of r_s the curves are even more similar. Taking all this together we arrive at the conclusion that it is indeed possible to use the Clark-Westhaus form for the energy in a quantitatively accurate manner provided one uses a sufficiently refined form for the three-body distribution function like Eqs. (20) and (21). It is well justified to use the convolution form only in the minimization and calculate perturbative corrections to the energy from Eq. (21).

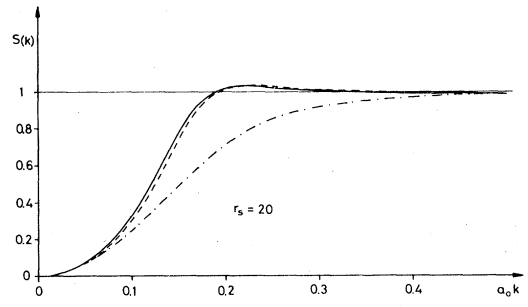

FIG. 2. Structure factor $S(k)$ for charged bosons at $r_s = 20$ from solution of Euler-Lagrange equation. Solid line, Clark-Westhaus form for the kinetic energy used. Dashed line, Jackson-Feenberg form used. Dot-dashed line, mean spherical approximation.

For completeness the last three columns of Table I give the model energy, obtained from the Bose version of Eqs. (50) to (53), the value of the radial distribution function at the origin, and the energy obtained from the mean spherical approximation,

$$S^{\mathrm{MSA}}(k) = k^2 \left(\frac{\hbar^2}{16 m \pi e^2 \rho} \right)^{1/2} \left(1 + \frac{\hbar^2}{16 m \pi e^2 \rho} k^4 \right)^{-1/2} ,$$

the Bose version of Eq. (44). This energy will become exact in the high-density limit but obviously the MSA cannot deal with strongly correlated systems like Coulomb fluids in the low-density limit.

B. Fermion fluid

The fermion electron fluid is characterized by the density and by the number of electrons in a given plane-wave state of the model determinant. In this section I will consider either two particles in a single plane-wave state, i.e., a spin unpolarized system with total spin zero, or a totally spin polarized system having total spin $N\hbar/2$ where only one electron is present in each state all electrons having the same spin projection. The only difference between these two systems in this formalism is the connection between density and Fermi momentum, Eq. (13), and the corresponding difference in the free Fermi-gas structure factor S_F. In Table II I present correlation and total energies for both cases as functions of r_s. These results follow from numerical solutions of Eq. (31) and evaluation of the energy from Eqs. (7) and (18)–(20) for ϵ_c^{CA} and addition of Eq. (21) for ϵ_c. It is seen that the corrections arising from the power-series expansion of the three-body distribution function, Eq. (15), are even smaller than in the Bose case never exceeding a millirydberg. In the case of the polarized fluid the "uncorrelated" state ϕ already incorporates quite strong statistical correlations due to the Pauli exclusion principle. Therefore the correlation energies due to dynamical correlations are almost a factor of 2 smaller than for the unpolarized system. From Eq. (45) it is easily calculated that this factor will become exactly equal to two in the limit $r_s \to 0$ which is also true for the RPA. The mean spherical approximation which will have the same limit as the other correlation energies for $r_s \ll 1$ is not very accurate even in the metallic density range $1 \leq r_s \leq 8$. At high densities the polarized system has a Fermi energy T_ϕ larger than the unpolarized system by a factor of $2^{2/3} \approx 1.587$, resulting in the total energy being larger by a comparable amount since the Fermi energy becomes dominant in this limit.

The results in the upper half of Table II are in excellent agreement with those obtained by Stevens and Pokrant[18] using the same variational method in conjunction with the convolution or superposition ap-

TABLE II. Correlation and total energies for the spin polarized and unpolarized electron fluids, in rydberg units. Same notation as Table I. ϵ_c, correlation energies; E, total energy. Note that $g(r=0)=0$ for the spin polarized fluid.

			Unpolarized			
r_s	$\epsilon_C^{\mathrm{MSA}}$	$\epsilon_C^{\mathrm{CW\text{-}CA}}$	ϵ_C	$\epsilon_C^{\mathrm{MOD}}$	E	$g(r=0)$
1	−0.1465	−0.1135	−0.1141	−0.1135	+1.1795	0.304
2	−0.1156	−0.0852	−0.0859	−0.0850	+0.0083	0.202
3	−0.0990	−0.0703	−0.0710	−0.0700	−0.1309	0.143
4	−0.0881	−0.0605	−0.0612	−0.0602	−0.1522	0.105
5	−0.0801	−0.0535	−0.0541	−0.0531	−0.1490	0.081
8	−0.0648	−0.0404	−0.0409	−0.0400	−0.1210	0.044
10	−0.0583	−0.0350	−0.0355	−0.0346	−0.1051	0.032
14	−0.0493	−0.0279	−0.0282	−0.0275	−0.0824	0.020
16	−0.0460	−0.0254	−0.0257	−0.0250	−0.0744	0.017
20	−0.0409	−0.0216	−0.0218	−0.0213	−0.0621	0.013
24	−0.0370	−0.0189	−0.0191	−0.0185	−0.0534	0.010
28	−0.0340	−0.0168	−0.0169	−0.0165	−0.0468	0.009
32	−0.0315	−0.0152	−0.0153	−0.0149	−0.0418	0.007
36	−0.0295	−0.0138	−0.0139	−0.0136	−0.0377	0.006
40	−0.0277	−0.0127	−0.0128	−0.0125	−0.0343	0.006

			Polarized		
r_s	$\epsilon_C^{\mathrm{MSA}}$	$\epsilon_C^{\mathrm{CW\text{-}CA}}$	ϵ_C	$\epsilon_C^{\mathrm{MOD}}$	E
1	−0.0956	−0.0544	−0.0547	−0.0545	+2.2986
2	−0.0784	−0.0413	−0.0416	−0.0413	+0.2581
3	−0.0689	−0.0345	−0.0348	−0.0345	−0.0299
4	−0.0624	−0.0301	−0.0303	−0.0301	−0.0997
5	−0.0576	−0.0269	−0.0271	−0.0269	−0.1178
8	−0.0481	−0.0210	−0.0212	−0.0209	−0.1107
10	−0.0439	−0.0185	−0.0186	−0.0184	−0.0990
14	−0.0379	−0.0151	−0.0152	−0.0151	−0.0798
16	−0.0357	−0.0139	−0.0140	−0.0139	−0.0725
20	−0.0322	−0.0121	−0.0121	−0.0120	−0.0610
24	−0.0295	−0.0107	−0.0107	−0.0106	−0.0527
28	−0.0273	−0.0096	−0.0096	−0.0096	−0.0464
32	−0.0255	−0.0088	−0.0088	−0.0087	−0.0415
36	−0.0240	−0.0081	−0.0081	−0.0080	−0.0375
40	−0.0227	−0.0075	−0.0075	−0.0074	−0.0342

proximation to g_3 and a parametrized correlation factor $f(r)$, Eq. (1). The solution of the Euler-Lagrange equation (31) does not improve the energy within the number of digits given. This is another example of the astounding insensitivity[13] of variational methods to the correlation factor used. In Fig. 3 the correlation factors, more precisely the pseudopotentials are compared. The correct $k \to 0$ limit is built into the pseudopotential used by Stevens and Pokrant

$$u(r) = -e^2(4\pi\rho e^2\hbar^2/m)^{-1/2}r^{-1}(1-e^{-br}) \quad , \qquad b = 0.92k_F \text{ at } r_s = 5 \tag{62}$$

so that both functions must agree for small k. But even for rather large values of momentum the

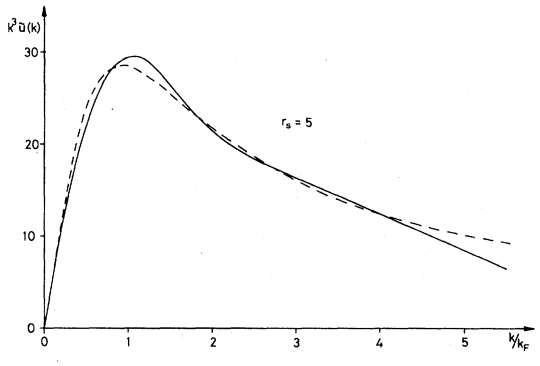

FIG. 3. Fourier transforms of the optimal (solid line) and parametrized (dashed line) pseudopotentials at $r_s = 5$.

analytical function is remarkably close to the optimal one calculated from the Euler-Lagrange equation. The only appreciable difference arises in the large-k limit, but this difference is not large enough to affect the first four digits of the energy in spite of this $u(r)$ violating the cusp condition (see Sec. II F) since $u'(0) \neq a_0$.

Stevens and Pokrant also performed calculations using different pseudopotentials for spin-parallel and spin-antiparallel electron pairs.[18] They did not find any decrease in the variational energy by allowing for this additional flexibility. It was therefore not thought worthwhile to incorporate such flexibility in the present treatment. Moreover, their finding confirms the statement made in Sec. II A that spin-dependent correlations are not important for the present problem.

Perturbational theories of the electron fluid, in particular, the RPA, are frequently plagued by negative $g(r)$ for small r and sufficiently large r_s. The same holds true for the mean spherical approximation as the reader may easily convince himself by taking the Fourier transform of Eq. (44) for not too small r_s. On the other hand *any* hypernetted-chain variational theory necessarily results in strictly positive radial distribution functions. This may easily be seen from Eq. (11) or Eq. (26) where a logarithm of $g(r)$ occurs which is not defined for nonpositive $g(r)$. It is also easy to see how the Euler-Lagrange equation (31) manages to keep $g(r)$ away from too small (positive) values: The matrix D_{lk}, Eq. (32), contains a term $g(r)^{-1}$ which will become infinitely large for $g(r)$ approaching zero. This term will then act in Eq. (31) to drive $g(r)$ away from this region.

In Fig. 4(a) radial distribution functions for the unpolarized electron fluid are shown at various densities. Strong correlations in the low-density limit are obvious. Therefore any perturbational treatment will eventually become doubtful for sufficiently large values of r_s. For variational methods, however, this limit is "easier" than the high-density limit since any approximation done in the treatment of Fermi statistics will become negligible.

Also shown in Fig. 4(a) are some results from Ceperley's variational Monte Carlo calculation,[1,30] which amounts to a straight evaluation of the multidimensional integral Eq. (2). The present theory agrees well with his values for the radial distribution function. It is to be noted that the statistical error bars inherent in the Monte Carlo results become quite large with r approaching zero.

In Fig. 4(b) radial distribution functions are shown

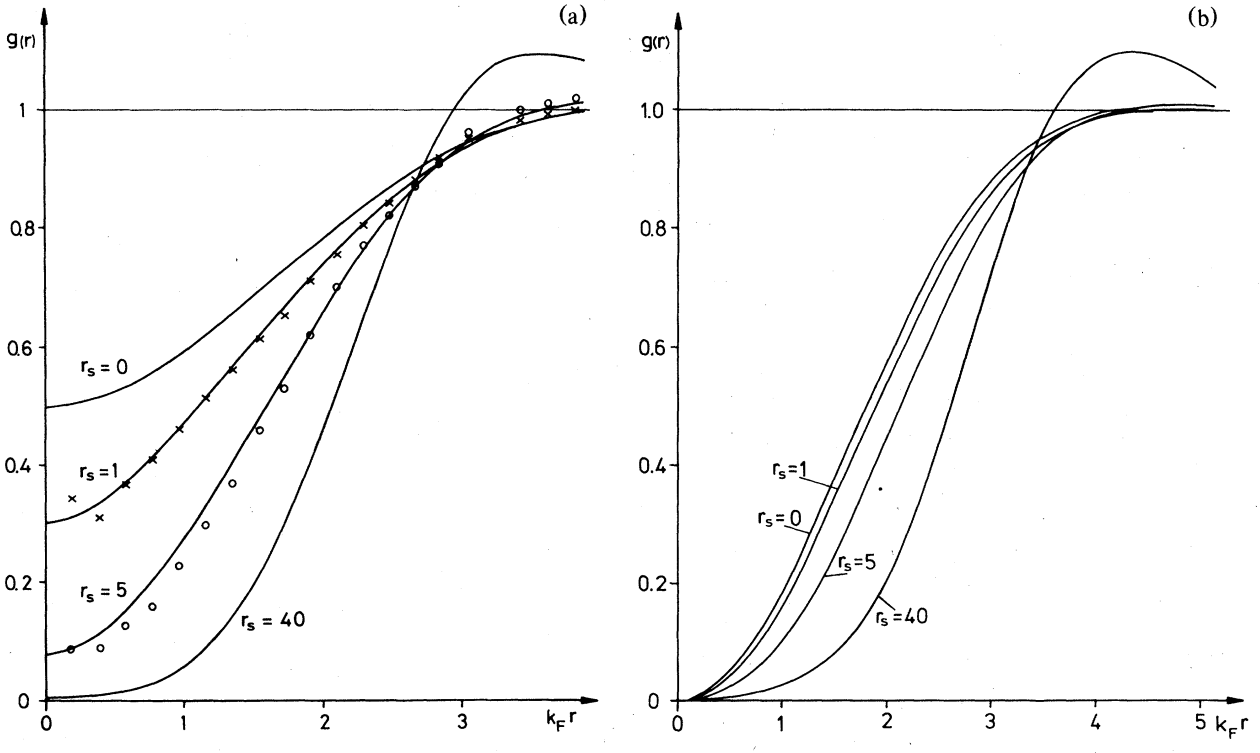

FIG. 4. (a) Radial distribution functions from the present calculation, unpolarized fluid. ×, Monte Carlo variational calculation of Ref. 1 at $r_s = 1$. ○, Monte Carlo variational calculation of Ref. 1 at $r_s = 5$. (b) Same as Fig. 4(a), spin polarized fluid.

for the spin polarized fluid. At the origin, $g(r)=0$ exactly sine the Pauli principle forbids two identical particles to be at the same point. In the present approach this property is maintained exactly since the first term of the product [Eq. (24)] vanishes whenever two particles come together, manifesting itself in a logarithmic divergence of the function $w(r)$, Eq. (25), at the origin as a consequence of the free Fermi-gas distribution function $g_F(r=0)=0$.

In the high-density or $r_s \to 0$ limit perturbational methods and, in particular, the RPA become exact. The radial distribution function tends towards the free one shown as the limit $r_s=0$ in Fig. 4. It is this limit which is rather difficult to treat for variational methods. This is because these methods and the approximations involved have been designed for strongly interacting systems as opposed to this weakly interacting limit, and motivates the extensive discussion of this limit in Sec. II where it was shown that this limit is treated correctly by the present method with the reservation made about state dependence.

The variational wave function (1) explicitly neglects state dependence of the correlation factors. It was shown in Sec. II C that this choice of trial wave function leads to an upper bound 8.4% above the exact correlation energy as $r_s \to 0$. It remains to be discussed how much the results in more interesting density regimes are affected. In Table III correlation energies from various theories of the electron fluid are compared. The sixth column gives variational Monte Carlo results[1] obtained with a wave function of the form Eq. (1) but using parametrized correlation factors $f(r)$. Therefore, this calculation should yield the same 8.4% difference to the exact $r_s \to 0$ limit as the present treatment. Recently Ceperley has been able to solve Schrödinger's equation for the ground state of the electron fluid by means of the Green's-function–Monte Carlo technique.[30,31] Corresponding correlation energies are given in the seventh column of Table III. To within a statistical error of one unit in the last digit given, the numbers represent the exact eigenvalue of the Schrödinger equation. Unfortunately such results are not available at present for $r_s < 1$. At $r_s=5$ the exact Shrödinger eigenvalue is two millirydberg below the upper bound obtained from the Jastrow wave function (1). Also the agreement with the nonvariational coupled-cluster theory,[4] column five, is of the same order. The results from the present treatment, fourth column, are seen to be upper bounds in all cases. The differences from the variational Monte Carlo results are of the order of one millirydberg for $r_s > 2$. Since the present results agree to within all digits given with those obtained by Stevens and Pokrant[18] who use a parametrized correlation factor it is fair to assume that the difference is totally due to the HNC approximation used here. The differences from the exact eigenvalues are of the order of a few millirydberg. It is interesting to note in this context that the present method needs only about one hundredth of the computer time used in the Monte Carlo method, specifically about 3 min/density on a CDC 7600. The last column gives the results from Lantto and Siemens[2] using the Fantoni-Rosati Fermi-HNC method. In spite of the variational character of this calculation these results do not seem to be upper bounds to the exact eigenvalue. At $r_s=1$ their result is significantly—more than 10%—not only below the Monte Carlo variational upper bound and similarly below most other recent calculations, but also below the exact Schrödinger eigenvalue obtained from the GFMC (Green's function Monte Carlo) method. In face of the long-range difficulty pointed out by Krotscheck[7] it would be extremely interesting to find the $r_s \to 0$ behavior of this theory, which has not been possible so far.

Another, very promising approach leading to a still different version of Fermi-hypernetted-chain Euler-

TABLE III. Comparison of correlation energies for the unpolarized fluid from various authors. LS-FR, variational FHNC, from Ref. 2; GFMC, exact Schrödinger eigenvalue by Green's function Monte Carlo, Ref. 30; VMC exact upper bound by variational Monte Carlo, Ref. 1; CC(2), nonvariational, partially summed perturbationally, coupled-cluster theory, Ref. 4; RPA, Ref. 23; remaining columns, present work, same notation as Tables I and II. Energies in rydberg units.

r_s	$\epsilon_C^{\mathrm{RPA}}$	$\epsilon_C^{\mathrm{MSA}}$	ϵ_c	$\epsilon_C^{\mathrm{CC(2)}}$	$\epsilon_C^{\mathrm{VMC}}$	$\epsilon_C^{\mathrm{GFMC}}$	$\epsilon_C^{\mathrm{LS\text{-}FR}}$
$\to 0$	$0.0622 \ln r_s$	$0.0570 \ln r_s$	$0.0570 \ln r_s$	$0.0622 \ln r_s$	$(0.0570 \ln r_s)$	$(0.0622 \ln r_s)$	?
1	−0.1576	−0.1465	−0.1141	−0.123	−0.122	−0.122	−0.138
2	−0.1236	−0.1156	−0.0859	−0.0917	−0.0874	−0.0902	−0.098
3	−0.1055	−0.0990	−0.0710	−0.0751	−0.0722	···	−0.079
4	−0.0936	−0.0881	−0.0612	−0.0644	−0.0624	···	−0.067
5	−0.0849	−0.0801	−0.0541	−0.0568	−0.0550	−0.0563	−0.058
10	−0.0613	−0.0583	−0.0355	···	−0.0363	−0.0372	−0.037
20	−0.0428	−0.0409	−0.0218	···	−0.0225	−0.0230	···

TABLE IV. Same as Table III but for totally spin polarized fluid.

r_s	ϵ_C	$\epsilon_C^{\mathrm{VMC}}$	$\epsilon_C^{\mathrm{GFMC}}$
$\rightarrow 0$	$0.0285 \ln r_s$	$(0.0285 \ln r_s)$	
1	−0.0547	−0.0582	
5	−0.0271	−0.0303	−0.0311
10	−0.0186	−0.0208	−0.0209
20	−0.0121	−0.0135	−0.0136

Lagrange equations is due to Owen.[32] Unfortunately no results are available so far for the electron fluid.

The fifth column of Table III gives results from Bishop and Lührmann's coupled-cluster calculation[4] representing the currently most advanced partially summed perturbation-theory approach the lowest order of which is the RPA. Their calculation is nonvariational, therefore, and extremely close to the exact Schrödinger eigenvalue.[30]

Table IV shows a comparison of present results with Ceperley's variational Monte Carlo calculation,[1] for the spin polarized (ferromagnetic) state. The agreement is not as nice as it is for the unpolarized case. However, the difference is never larger than 10%. The variational Monte Carlo results are even closer to the corresponding exact Shrödinger eigenvalues from a Green's-function–Monte Carlo calculation[30] than in the unpolarized case. I conclude that the present method yields correlation energies not more than a few millirydberg above the exact value. This could already have been inferred from the comparison of variational and model energies in Table II which should be a measure of this difference, see Sec. II D, and from the agreement with the nonvariational coupled-cluster energies in Table III for the unpolarized case.

C. Low-density and Bose limits

At very low densities interacting electrons become classical. Therefore it must become less and less important with decreasing density whether the electrons are considered as Bose, Fermi, or Boltzmann particles. Moreover, since there is no spin-spin interaction in the present Hamiltonian, spin polarization must become negligible in this limit for the same reason. In Table V present results are collected for these three cases and compared to corresponding variational Monte Carlo results.[1] The energies shown in Table V are *total* energies per particle, *not* correlation energies since only total energies will become equal in the low-density limit which is nicely exhibited. Since I start from a plane-wave determinant, all results of the present treatment pertain to a fluid phase. On the other hand it is very well known that at low densities electrons will crystallize. The second column of Table V therefore gives total energies per electron from the anharmonic-crystal calculation of Carr *et al.*[33] It is seen that in this density regime crystal and fluid energies are extremely close which renders determination of the density where the phase transition occurs very difficult.

It is seen from Table V that the two Fermi fluid energies become equal to each other more rapidly than they become equal to the Bose fluid energy, as should be expected. Ceperley[1] even finds a crossover point in his variational study, i.e., lower energies for the polarized than for the unpolarized phase for $r_s > 26$. This does not occur in the present calculation. However, the differences between polarized and unpolarized ground-state energies are smaller than the uncertainty due to the approximation to g_3 for low densities so that these differences are not significant.

The second and third columns of Table III give the RPA and MSA correlation energies. While the RPA becomes exact for $r_s \rightarrow 0$ and the MSA becomes an upper bound both analytical solutions yield energies well below the exact value for interesting values of r_s. It is to be noted, however, that in spite of its simplic-

TABLE V. Comparison of present total energies per electron with low-density expansion of Ref. 33. Energies in rydberg units. E_{FHNC}—present work, E_{VMC}—from Ref. 1, E^{CRYST}—from Ref. 33.

r_s	E^{CRYST}	$E_{\mathrm{FHNC}}^{\mathrm{FLUID}}(P=0)$	$E_{\mathrm{VMC}}^{\mathrm{FLUID}}(P=0)$	$E_{\mathrm{FHNC}}^{\mathrm{FLUID}}(P=1)$	$E_{\mathrm{VMC}}^{\mathrm{FLUID}}(P=1)$	$E_{\mathrm{BOSE}}^{\mathrm{FLUID}}$
20	−0.0618	−0.0621	−0.0628	−0.0610	−0.0624	−0.0659
32	−0.0421	−0.0418	−0.0422	−0.0415	−0.0425	−0.0433
36	−0.0381	−0.0377	−0.0383	−0.0375	−0.0384	−0.0389
40	−0.0348	−0.0343	−0.0348	−0.0342	−0.0350	−0.0353

ity and neglect of state dependence the MSA nevertheless is always closer to the exact eigenvalue except for $r_s \ll 1$.

In Fig. 5 I compare the integrands for the model energies, Eq. (50), from various theories for the case $r_s = 1$. It has been shown in Sec. II D that the low momentum limits of these functions must agree. It is interesting to note that it is pronouncedly in the large momentum limit that the complete theories, HNC and coupled cluster, yield similar behavior quite different from the behavior found for the analytical RPA and MSA. In spite of the rather similar integral—the correlation energy—the integrands obtained from HNC and coupled-cluster theories look somewhat different. In the variational treatment, contributions to the correlation energy come more pronouncedly from large values of the momentum transfer whereas in the coupled-cluster theory correlation energy is gained more pronouncedly from smaller values of the momentum transfer.

It is obvious that the analytical theories RPA and MSA fail quite badly for large momenta and consequently overbind. However, the MSA is more accurate specifically for momenta above the Fermi momentum.

As stated in Sec. II D the difference between model and variational energy should be a measure of the "distance" between the Jastrow-type wave function (1) and the true ground-state wave function. This difference is significantly smaller in the polarized than in the unpolarized case, signalling that the Jastrow wave function is "better" in the polarized case. If one finds lower variational energies for the polarized phase this might merely reflect the better quality of the wave function used and need not signal a physical phase transition.

Comparing the crystalline, Fermi fluid, and Bose fluid energies of Table V it is to be noted that though numerically quite similar these energies are of quite different origin. For all cases, kinetic energy is negligible. The crystalline and Bose fluid energies almost entirely consist of potential energy all of which comes from correlations in the Bose fluid case whereas it is all electrostatic for the crystalline case. The Fermi fluid energies are made up from a larger exchange

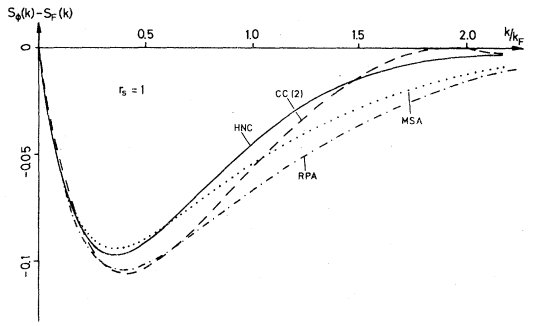

FIG. 5. Integrands for the model energy, $S_\phi - S_F$, Eq. (50). CC(2), from Ref. 4; RPA, from Ref. 23.

energy and a smaller correlation energy contribution as may be seen by comparing with Table II. Of course, this is nothing but an exemplification of the triviality that "exchange" and "correlation" terms are only defined with reference to an "unperturbed" state.

It might look rather surprising that the fluid wave function Eq. (1) is capable of describing a state very close to a solid in energy. However, the Jastrow correlation factor does build strong many-body correlations into the system. On the two-body level this is exhibited by the distribution functions of Fig. 4. It has even been argued[34] that an actual crystal could accurately be described by a translationally invariant wave function like Eq. (1)—the floating crystal model.

D. Variable polarization

For applications it is useful to know correlation energies not only as functions of density but also as functions of spin polarization P. In Table II I presented results for the unpolarized $P = 0$ electron fluid and for the totally polarized fluid, $P = 1$. An interpolation formula widely in use has been given by von Barth and Hedin[6]

$$\epsilon_C(r_s,P) = \epsilon_C(r_s,P=0) + [\epsilon_C(r_s,P=1) - \epsilon_C(r_s,P=0)]\{[\tfrac{1}{2}(1+P)]^{4/3} + [\tfrac{1}{2}(1-P)]^{4/3} - 2^{-1/3}\}/(1-2^{-1/3}) \quad . \quad (63)$$

In order to check the above interpolation formula I performed several calculations using specific intermediate values for the polarization. This is easily done within the present formalism since the only place where spin polarization enters is the uncorrelated state ϕ. The correlation factor will be adjusted by solution of the Euler-Lagrange equation (31). The only knowledge required to carry through this program is the noncorrelated distribution function or structure function entering Eq. (31). For the present case this is, $\pm$ denoting spin up or down,

TABLE VI. Correlation energy as function of spin polarization and density. ϵ_C (interpol.), from Eq. (63); $\epsilon_C(P)$, from solution of Eq. (31). Energies in rydberg units.

r_s	ϵ_c (interpol.)	ϵ_c ($P=0.3228$)	ϵ_c ($P=0$)	ϵ_c ($P=1$)
1	−0.1088	−0.1084	−0.1141	−0.0547
5	−0.0517	−0.0516	−0.0541	−0.0271
10	−0.0340	−0.0339	−0.0355	−0.0186
20	−0.0209	−0.0210	−0.0218	−0.0121

Fermi momenta

$$k_{F\pm}=[3\pi^2\rho(1\pm P)]^{1/3} \ .$$

Slater functions, with j_1 a spherical Bessel function

$$l_{\pm}(r)=(3/k_{F\pm}r)j_1(k_{F\pm}r) \ .$$

Radial distribution function

$$g_F(r)=1-\sum_{\pm}\tfrac{1}{4}(1\pm P)^2 l_{\pm}(r)$$

from which the structure function S_F may be obtained by Fourier transformation.

In Table VI the approximate interpolation formula is compared to actual minimization of the variational energy. It is seen that the error of the interpolation formula is always less than a millirydberg. Similar results obtain at other polarizations and densities.

IV. SUMMARY

The present paper continues investigations on the Jastrow variational method as applied to the electron fluid. Within the framework of the hypernetted-chain approximation accurate variational upper bounds to the ground-state energy are obtained. After doing approximations the theory still behaves correctly in the high- and low-density limits and in the long-wavelength limit. The only exception to this statement is the neglect of state dependence in the correlation factor in the very ansatz for the wave function, Eq. (1), which leads to an upper bound 8.4% above the exact correlation energy in the high-density limit but not to serious underestimation of the energy in the metallic density regime. By comparison with Monte Carlo results it is seen that the hypernetted-chain variational upper bound is of the order of one millirydberg above the exact expectation value, and only a few millirydberg above the exact ground-state energy in the metallic density range. Furthermore, it is found that the Jastrow-type wave function (1) is closer to the exact ground-state wave function for the spin polarized fluid than for the spin unpolarized fluid as evidenced by the comparison with model energies. Variational least upper bounds within the space of functions (1) have been computed for a variety of densities and polarizations.

In the high-density limit an analytical solution of the Euler-Lagrange equation, the mean spherical approximation, has been obtained. The analytical form is much simpler than the one obtained from the RPA[23] and the derivation is much less demanding. Nevertheless, the correlation energies obtained from this approximation are always closer to the exact ones than the ones obtained from the RPA with the exception of $r_s \ll 1$ where the neglect of state dependence becomes important.

The present variational treatment of fermion fluids immediately extends to other than Coulombic forces. Nowhere but in the evaluation of asymptotic properties was made use of the special case of the Coulomb interaction. The central equations (5), (9), (18)–(21), and (31) apply to any other central interaction $v(r)$ without alteration. The asymptotic properties of $S(k)$ may be obtained from Eq. (35) by just replacing the potential function $v(k)$ in the first term. Numerical calculation bears out that the present treatment gives results for superpositions of Yukawa potentials in very good agreement with other treatments.[13]

ACKNOWLEDGMENTS

Many thanks are due to P. Bodden, D. Ceperley, J. W. Clark, B. D. Day, K. Emrich, M. Kalos, E. Krotscheck, J. Kübler, K. H. Lührmann, J. C. Owen, and P. J. Siemens for illuminating discussions as well as making results available before publication. The kind hospitality of the Argonne National Laboratory where the major part of this work was performed is gratefully acknowledged. Work performed under the auspices of the U.S. DOE and supported by the Deutsche Forschungsgemeinschaft.

*Present and permanent address: Institut für Theoretische Physik, Ruhr-Universität Bochum, D-4630 Bochum 1, West Germany.

[1]D. Ceperley, Phys. Rev. B 18, 3126 (1978).
[2]L. J. Lantto and P. J. Siemens, Nucl. Phys. A 317, 55 (1979); L. J. Lantto, Nucl. Phys. A 328, 297 (1979).
[3]S. Fantoni and S. Rosati, Nuovo Cimento 25, 593 (1975).
[4]R. F. Bishop and K. H. Lührmann, Phys. Rev. B (in press).
[5]W. Kohn and L. J. Sham, Phys. Rev. 140, A1133 (1965); L. Hedin and B. I. Lundqvist, J. Phys. C 4, 2064 (1971).
[6]U. v. Barth and L. Hedin, J. Phys. C 5, 1629 (1972); O. Gunnarsson and B. I. Lundqvist, Phys. Rev. B 13, 4274 (1976).
[7]E. Krotscheck and M. L. Ristig, Nucl. Phys. A 242, 389 (1975); 293, 293 (1977).
[8]A. Bijl, Physica (Utrecht) 7, 869 (1940); R. B. Dingle, Philos. Mag. 40, 573 (1949); R. Jastrow, Phys. Rev. 98, 1479 (1955).
[9]P. A. Whitlock, D. M. Ceperley, G. V. Chester, and M. H. Kalos, Phys. Rev. B 19, 5598 (1979).
[10]E. Feenberg, *Theory of Quantum Fluids* (Academic, New York, 1969).
[11]J. W. Clark and P. Westhaus, Phys. Rev. 141, 833 (1966); 149, 990 (1966).
[12]J. G. Zabolitzky, Phys. Rev. A 16, 1258 (1977).
[13]J. G. Zabolitzky, Adv. Nucl. Phys. (in press).
[14]J. M. J. van Leeuwen, J. Groeneveld, and J. de Boer, Physica (Utrecht) 25, 792 (1959); T. Morita, Prog. Theor. Phys. 20, 920 (1958).
[15]J. W. Clark, Prog. Part. Nucl. Phys. 2 (1979).
[16]F. Lado, J. Chem. Phys. 47, 5369 (1967).
[17]M. A. Pokrant and F. A. Stevens, Jr., Phys. Rev. A 7, 1630 (1973); M. S. Becker, A. A. Broyles, and T. Dunn, Phys. Rev. 175, 224 (1968).
[18]F. A. Stevens, Jr., and M. A. Pokrant, Phys. Rev. A 8, 990 (1973).
[19]D. Pines and P. Nozieres, *Theory of Quantum Liquids* (Benjamin, New York, 1966).
[20]A. D. Jackson, A. Lande, and L. J. Lantto, Nucl. Phys. A 317, 70 (1979).
[21]J. A. Barker and D. Henderson, Rev. Mod. Phys. 48, 587 (1976).
[22]I. S. Gradshteyn and I. M. Ryzhik, *Tables of Integrals, Series and Products* (Academic, New York, 1965).
[23]R. F. Bishop and K. H. Lührmann, Phys. Rev. B 17, 3757 (1978).
[24]J. C. Owen (private communication).
[25]H. G. Kümmel, Z. Phys. 279, 271 (1976).
[26]K. Emrich and J. G. Zabolitzky (unpublished).
[27]H. W. Jackson and E. Feenberg, Ann. Phys. (N.Y.) 15, 266 (1961).
[28]L. J. Lantto and R. M. Nieminen, Phys. Lett. A 66, 106 (1978).
[29]D. K. Lee and F. H. Ree, Phys. Rev. A 5, 814 (1972).
[30]D. Ceperley (private communication) and (unpublished).
[31]D. M. Ceperley and M. H. Kalos, in *Topics in Current Physics*, edited by K. Binder (Springer, Heidelberg, 1979), Vol. 7.
[32]J. C. Owen (unpublished).
[33]W. J. Carr, R. A. Coldwell - Horsfall, and A. E. Fein, Phys. Rev. 124, 747 (1961).
[34]E. Feenberg, J. Low Temp. Phys. 16, 125 (1974).